Pangenome analysis of the soil-borne fungal phytopathogen *Rhizoctonia solani* and development of a comprehensive web resource: RsolaniDB

Kaushik, A.[1], Roberts, D.P.[2], Ramaprasad A.[1], Mfarrej, S.[1], Mridul Nair[1], Lakshman, D.K.*[2] and Pain, A.*[1,3]

[1]Biological & Environmental Science & Engineering Division, KAUST, Thuwal 23955-6900, Saudi Arabia

[2]Sustainable Agricultural Systems Laboratory, USDA-ARS, Beltsville, MD 20705, USA

[3]Research Center for Zoonosis Control, Global Institution for Collaborative Research and Education (GI-CoRE); Hokkaido University, Sapporo, 001-0020 Japan

* Corresponding authors

Abstract

Rhizoctonia solani is a collective group of genetically and pathologically diverse basidiomycetous fungus that damages economically important crops. Its isolates are classified into 13 Anastomosis Groups (AGs) and subgroups having distinctive morphology and host range. The genetic factors driving the unique features of *R. solani* pathology are not well characterized due to the limited availability of its annotated genomes. Therefore, we performed genome sequencing, assembly, annotation and functional analysis of 12 *R. solani* isolates covering 7 AGs and selected subgroups (AG1-IA, AG1-IB, AG1-IC, AG2-2IIIB, AG3-PT (isolates Rhs 1AP and the hypovirulent Rhs1A1), AG3-TB, AG4-HG-I (isolates Rs23 and R118-11), AG5, AG6, and AG8), in which six genomes are reported for the first time, wherein we discovered unique and shared secretomes, CAZymes, and effectors across the AGs. Using a pangenome comparative analysis of 12 *R. solani* isolates and 15 other basidiomycetes, we also elucidated the molecular factors potentially involved in determining the AG-specific host preference, and the attributes distinguishing them from other Basidiomycetes. Finally, we present the largest repertoire of *R. solani* genomes and their annotated components as a comprehensive database, viz. RsolaniDB, with tools for large-scale data mining, functional enrichment and sequence analysis not available with other state-of-the-art platforms, to assist mycologists in formulating new hypotheses.

Introduction

Rhizoctonia solani Kühn (teleomorph: *Thanatephorus cucumeris* [Frank] Donk) is considered as one of the most destructive soil borne plant pathogens causing various diseases including pre- and post-emergence damping-off of seedlings, crown and root rots, black scurf of potato, take-all of wheat, sheath blight of rice and maize, brown patch of turf, and postharvest fruit rots (1, 2). This necrotrophic fungus infects a wide range of economically important plant species, belonging to more than 32 plant families and 188 genera, and is responsible for 15% to 50% agricultural damages annually (3). Broadly, it is classified among 13 Anastomosis Groups (AGs) with distinctive morphology, physiology, pathogenicity host range, and highly divergent genetic composition (4). Most *R. solani* AGs are further divided into subgroups, also called IntraSpecific Groups (ISGs), which differ in pathogenicity, virulence, ability to form sclerotia, growth rate, and host range preference (5). Although field isolates of *Rhizoctonia* infected plants are usually found to be infested with one or more AGs, each AG subgroup can still have its own host preference. For instance, *Arabidopsis thaliana*, was found to be susceptible to AG2-1 sub-group isolates but resistant to AG8 isolates (6), which suggests that genetic divergence is the inherent characteristic of *Rhizoctonia* species.

Over the last two decades, our understanding of the genetic divergence among different *R. solani* AGs has improved to the point that it is now evident that all AGs and their sub-groups are genetically isolated, non-interbreeding populations (7). The rapid and relatively low-cost of generation of genomic sequences and other '*omics*' datasets has played a significant role in furthering our understanding of the host-pathogen interactions and ecology of *Rhizoctonia* species. (8–12). The analysis of these genomic sequences and functional components revealed several novel or previously unrecognized classes of *R. solani* genes among different AGs that are

involved in pathogenesis in a host-specific manner, e.g. effector proteins and carbohydrate-active enzymes (CAZymes) (13). Additionally, analysis of differentially expressed genes in different isolates has enabled researchers to predict the adaptive behavior of this fungus in different hosts and the associated virulence (14, 15). However, the majority of this information has come from the analysis of isolates belonging to only a small number of AGs for which complete genome and/or transcriptome sequences are available. In fact, until now, draft genome assemblies belonging to only 4 of the 13 AGs have been reported viz. AG1-IA (16), AG1-IB (17), AG2-2IIIB (13), AG3-Rhs1AP (18), AG3-PT isolate Ben-3 (19) and AG8 (20). This limited availability of genome sequences and the predicted proteomes across the 13 different AGs and their subgroups is one of the important barriers hindering the understanding of functional complexity and temporal dynamics in *R. solani* AGs and their subgroups.

In this study, we report whole-genome sequencing, assembly and annotation of 12 *Rhizoctonia* isolates from 7 AGs; of which genome sequences of three AGs (AG4, AG5, and AG6), two subgroups (AG1-IC and AG3-TB {or AG3-T5}) and a hypovirulent isolate (AG3-1A1) of the subgroup AG3-PT are being reported for the first time. The draft genome of the AG3-PT isolate 1AP (alternatively named as Rhs1AP) was previously reported (Cubeta et. al., 2014) (18), but was re-sequenced for comparative purposes, as AG3-1AP. Furthermore, to understand genetic diversity among different *R. solani* isolates, we performed inter-proteome comparative analyses, including ortholog analysis at the pangenome level and protein domains profiling for secreted components, virulent proteins, and CAZymes in all 12 *R. solani* isolates. To make these high-quality draft *R. solani* genomes and features readily accessible to a broad audience of researchers, we built a comprehensive and dedicated web resource, viz. RsolaniDB, for hosting and analyzing the available genomic information predicted at the transcript-, and

protein-level in different *R. solani* AGs. The presented web-resource includes detailed information on each *R. solani* isolate, such as the genome properties, predicted gene, transcript and protein sequences, predicted gene function, and protein orthologues among other AG sub-groups, along with tools for Gene Ontology (GO) and pathway enrichment analysis, sequence analysis, and visualization of gene models.

Materials and Methods

Isolation of genomic DNAs for sequencing

Details regarding *R. solani* isolates used for sequence analyses are presented in Table S1 and S2. Fungal cultures were purified by the hyphal tip excision method (21) and maintained by sub-culturing on potato dextrose agar (PDA, Sigma Aldrich catalog # P2182, St. Louis, MO, USA). The PDA was amended with kanamycin (25 µg/ml) and streptomycin (50 µg/ml) to inhibit bacterial growth. Isolates were grown in Potato Dextrose Broth (PDB, Sigma Aldrich catalog # P6685) broth at 100 rpm and 25 C for 4 to 6 days, mycelia collected by filtration through 2 layers of sterile cheese cloth, washed 2 X with sterile distilled water, gently squeezed and placed on 4 layers of paper towel to remove surface water, and then snap-frozen in liquid nitrogen and stored at -80 C till use. Genomic DNA was extracted from mycelia using both the CTAB method (22) and a protocol recommended by the manufacturer (User-Developed Protocol: Isolation of genomic DNA from plants and filamentous fungi using the QIAGEN® Genomic-tip, Qiagen Inc.). RNA was extracted from fungal isolates and from tobacco detached leaves infected with corresponding fungal isolates, using the Qiagen RNeasy Plant Mini Kit (Qiagen Inc. Germantown, MD, USA). Extracted genomic DNA and RNA was quantified with a Qubit Flex Fluorometer (Thermo Fisher Scientific, Waltham, MA, USA). AG and subgroup identity of the

104 fungal isolates was verified by ITS-PCR, sequencing and homology analysis with nucleotide
105 sequences available in the NCBI database (23).

106 **RNA extraction**

107 *Nicotina tabacum* seedlings were raised to four-leaf stage on potting mix (Pro-mix, Premier
108 Horticulture, USA) in the greenhouse at ambient temperature (22º - 24º C) and with four hours
109 supplemental light with a mercury lamp. Two leaves were excised from each seedling and placed
110 on a tray on two piece of wet paper towels. For inoculation, seven to eight agar plugs from the
111 margin of fresh *R. solani* growth on 1/4th concentration of PDA (potato dextrose agar) were
112 placed on the adaxial surface of each leaf. For control, only seven to eight agar plugs from 1/4th
113 PDA were placed. Each tray was closed with a lid and incubated on lab bench at ambient
114 temperature and light.
115 After 5 days, yellow to necrotic symptoms were noticeable on *R. solani* treated leaves but no
116 symptoms appeared on control leaves surrounding the plugs. The control and infected patches
117 were excised with a sterile scalpel, snap frozen in liquid nitrogen and processed for RNA
118 extraction with RNeasy Plus Mini Kit in RLC buffer (Qiagen Sciences Inc., Germantown, MD,
119 USA). The purified RNA was treated with DNase at 37º C for 30 min, extracted with phenol and
120 Phenol: chloroform, precipitated with ethanol, and dissolved in RNase-free water.

121 **Construction of genomic and RNA libraries and sequencing**

122 For making genomic libraries, an input of 500ng of DNA from each sample was sheared on
123 Covaris (Covaries E series) and paired-end libraries were prepared for sequencing using
124 Illumina's HiSeq 2000 platform. From end repair until adapter ligation and purification steps of
125 the paired-end libraries were prepared using the protocol "Illumina library prep" on the IP-Star
126 automated platform from Diagenonde (Diagenode IP Star) as per the manufacturer's protocol.

Post ligation, manual protocols were used for gel size selection and PCR amplification using the standard Illumina PCR Cycle (Kapa high-fidelity master mix). The prepared libraries were analyzed on bioanalyzer and quantified using Qubit (Thermo Fisher). The normalized libraries were pooled for sequencing (insert size of 500bp) and submitted for HiSeq 2000 sequencing at Bioscience Core Laboratory of King Abdullah University of Science and Technology. Strand-specific mRNA sequencing was performed from total RNA using TruSeq Stranded mRNA Sample Prep Kit LT (Illumina) according to manufacturer's instructions. Briefly, polyA+ mRNA was purified from total RNA using oligo-dT dynabead selection. First strand cDNA was synthesised using randomly primed oligos followed by second strand synthesis where dUTPs were incorporated to achieve strand-specificity. The cDNA was adapter-ligated and the libraries amplified by PCR. Libraries were sequenced in Illumina Hiseq2000 with paired-end 100bp read chemistry.

De novo assembly, genome annotation and bioinformatic analysis

Data preprocessing. Adapter sequences in genomic reads in FASTQ format were trimmed using the trimmomatic tool (version 0.35) (24), followed by trimming low-quality bases at read ends. Read quality was evaluated using the fastqc tool (version 0.11.8) (25). Reads with length < 20 bp and average quality score < 30 were also removed. For genome heterogeneity analysis, *k-mer* distribution analysis on resulting DNAseq reads was performed using jellyfish (version 2.2.10) (26), which estimated best *k-mer* length for each genome. Histogram distributions of different *k-mers* for the best *k-mer* length was plotted using the *-histo* module of the jellyfish program. In addition, the available raw RNAseq paired-end reads (Table S2) were quality trimmed and preprocessed using with the same approach used for DNAseq reads. The quality trimmed reads were then subjected to *denovo* assembly using Trinity which predicted transcript sequences (27).

Genome assembly. Quality trimmed reads were subjected to *denovo* genome assembly using SPAdes (version 3.7.0) in which a defined range of *k-mer* lengths (21,33,55,65,77,101 and 111) was used for contig formation (28). Quast (version 4.5) was used for quality evaluation of predicted contigs (29). Scaffolds were subsequently predicted from contigs using SSPACE (version3.0) (30) and gaps in assembled scaffolds filled using five consecutive runs of GapCloser (version 1.12) (31). For samples with RNAseq dataset available, genome scaffolding was further improved using the Rascaf program (32). Genome quality was evaluated with BUSCO (version 3.0.1) (33) and scaffolds subjected to ITSx (version 1.1) (34) for ITS sequence prediction. Thereafter, phylogenetic tree was constructed with megax software (35) using the neighborhood joining method (10000 bootstraps), in which ITS2 sequences were aligned using ClustalW (36). The resulting tree was saved in the newick format and visualized together using Phylogeny.IO (37) and ETE toolkit (38). Redundans python script was then used to predict the homozygous genome by reducing the unwanted redundancy to improve draft genome quality (39). Resulting scaffolds were aligned with mitochondrial genomes of *R. solani* and other Basidiomycota using blastn program (version 2.6.0; e-value $\leq 1e^{-5}$) (40) and mapped mitochondrial contigs were removed to retain only the nuclear genome for subsequent annotation.

Genome annotation. The draft genome was annotated using the MAKER (version 2.31.8) pipeline(41), which predicted intron/exon boundaries, transcript and protein sequences. For the annotation, repeat regions were masked using RepeatMasker (version 4.0.5; model_org=fungi) (42). Protein homology evidence was taken from UniProt protein sequences (Reviewed; family: Basidiomycota) (43). For EST evidences, RNAseq reads were assembled into transcripts using Trinity *denovo* assembler (version 2.0.6) (27). For genomic datasets without corresponding RNAseq datasets available, the EST sequences of alternate organisms were used from previously

published *R. solani* genome annotations viz. AG1-IA (16), AG1-IB (17), AG2-2IIIB (13), AG3-Rhs1AP (18), AG3-PT isolate Ben-3 (19) and AG8 (20). The functional domains, PANTHER pathways (44) and Gene Ontology (GO) terms (45) in the predicted protein sequences were assigned using InterProScan (version 5.45-80.0) standalone program (46). The functional domains assigned to each protein included the information from ProSiteProfiles (47), CDD (48), Pfam (49) and TIGRFAMs (50), resulting in the annotated genome in GFF3 format using iprscan2gff3 and ipr_update_gff programs (46).

The fungal AROM protein sequences were identified by mapping the *R. solani* proteome on pentafunctional AROM polypeptide sequences from UniProt (organism Fungi) using blastp (e-value $\leq$ 0.001) (40). The resulting candidate AROM sequences in each *R. solani* proteome were analyzed using HMMER webserver (51). We also identified the predicted secreted proteins in each of the *R. solani* proteomes using signalp (version 5.0) (52). For identification of proteins with a transmembrane domain phobius (version 1.01) (53) was used. We used targetp (version 1.1) to predict proteins with mitochondrial signal peptides (54). However, since we already removed mitochondrial contigs from assembled genomes, we did not observe any proteins with a mitochondrial signal peptide. Effector proteins in each *R. solani* secretome were predicted using effectorP webserver (version 2.0) (55). The Carbohydrate Active enZyme (CAZyme) in *R. solani* proteomes were predicted using dbCAN2 webserver, in which only the proteins predicted by at least two prediction methods were considered (56). The CAZyme family predicted by HMMER was used for the selected proteins.

Orthology. Orthologous proteins across all proteomes were identified with orthoMCL clustering using the Synima program (57, 58), which identified core, unique and auxiliary regions in each *R. solani* proteome. This program was also used for predicting genome synteny using inter-

196 proteome sequence similarity. ShinyCircos was used for circular visualization of synteny plots
197 (59, 60).

198 **RsolaniDB database development**

199 The RsolaniDB (RDB) database was built to host *R. solani* reference genomes, transcript and
200 protein sequences in FASTA format, along with genome annotations included in GFF3 format.
201 For each genome, the information in the database was structured as entries, in which each entry
202 included a list of details about a given transcript and protein, i.e., intron-exon boundaries;
203 predicted functions; associated pathways and GO terms; predicted sequences; orthologs and
204 functional protein sequence domains predicted from InterPro, PrositeProfile and Pfam. The
205 identifier format for each entry (i.e., RDB ID) start with 'RS_' and AG subgroup name followed
206 by a unique number. We also included five previously published *R. solani* annotated genome
207 sequences (i.e., AG1-1A, AG1-1B, AG2-2IIIB, AG3-PT and AG8) with their gene identifiers
208 converted into the RDB ID format. The database was written using DHTML and CGI-BIN Perl
209 and MySQL language, to allow users perform list of tasks, including text-based search for the
210 entire database; or in AG-specific manner. We also included a list of tools to assist users in
211 performing number of down-stream analysis, including RDB ID to protein/transcript sequence
212 conversion; FASTA sequence-based BLAST search on entire database or AG-specific manner;
213 tool to retrieve orthologs for a given set of RDB IDs along with tools for functional enrichment
214 analysis. The GO-based functional enrichment tool for gene set analysis of given RDB IDs was
215 build using topGO R package (61). Whereas the pathway-based gene set analysis was developed
216 to predict significantly enriched PANTHER pathway IDs for a given set of RDB IDs.

217 **Results**

218 **Genome-wide comparative analysis of *R. solani* assemblies and its annotation**

We performed the high-depth sequencing, *denovo* genome assembly and annotation of 12 *R. solani* isolates. For qualitative evaluation of these assemblies, we used genome sequences of a basidiomycetous mycorrhizal fungus *Tulasnella calospora* (Joint Genome Institute fungal genome portal MycoCosm (http://genome.jgi.doe.gov/Tulca1/Tulca1.home.htm) and *R. solani* AG3-PT as negative and positive controls, respectively. Overall, the draft genome assemblies of the *R. solani* isolates shows remarkable differences in the genome size, ranging anywhere from the smaller AG1-IC (~33 Mbp) to the larger AG3-1A1 (~71 Mbp) isolate genomes (Table S3). The number of contigs generated are also highly variable ranging between 678-11,793, in which the newly reported assemblies of AG1-IC and AG3-T5 has highest N50 lengths of 1,00,597 bp and 1,96,000 bp respectively (Table S3). The heterogeneity in genomic reads was predicted by analyzing the distribution of different *k-mers* in *R. solani* genomic sequencing reads. The analysis reveals a shoulder peak along with the major peak in *k*-mer frequencies for AG2-2IIIB, AG3-1A1, AG3-1AP and AG8, indicating the possible heterogeneity of these genomic reads of these isolates (Figure S1). The G+C content ranged from 47.47% to 49.07%, with a mean of 48.43% (Table S3). The quality of these draft genomes was evaluated using BUSCO with scores ranging between ~88-96% (Table S3), indicating the completeness of essential fungal genes in the predicted assemblies. In order to evaluate the reliability of the genome assemblies, we further compared our draft genomes with previously published assemblies of *R. solani* isolates, i.e., AG1-IA, AG1-IB, AG2-2IIIB, and AG8 (Figure S2). The mummer plot (62) comparison shows the overall co-linearity and high similarity among similar assemblies, wherein AG8 assemblies are least co-linear, possibly due to the heterokaryotic nature of the AG8 genome (20, 63). Among the presented draft genome sequences, a large number of syntenic relationships (Figure 1A) are also identified (length > 40,000bp), wherein all the given isolates share at least four highly

similar syntenic region, except *T. calospora* (outgroup), which does not share any syntenic region with *R. solani* isolated for the given threshold of > 40,000 bp (Figure 1B). Similarly, our analysis shows that AG5, AG2-2IIIB and AG3-1A1 shares comparatively lower syntenic regions, whereas AG3-PT (positive control) shares highest number of syntenic regions with other *R. solani* isolates. In fact, we observed that most of the closely related AGs share large number of syntenic relationships, e.g., high similarity among AG3 sub-groups. Overall, the analysis exhibits the first line of evidence that indicates widespread collinearity and regions of large similarity across genetically distinct isolates, with *T. calospora* as an outlier.

Subsequently, we performed the ITS2-based phylogeny to compare the ITS2 sequences of the 12 newly sequenced *R. solani* isolates with that of the known *R. solani* tester strains (as positive controls) and *T. calospora* as an outgroup (Figure 1C), wherein for AG3-PT, we were not able not predict the ITS sequences. The observed phylogenetic clusters of AGs reflect strong similarity in ITS2 sequences of assembled genomes with respect to that of tester strains of *R. solani*. For instance, the AG1-IA cluster includes four strains, all belonging to same AG, *i.e.*, AG1-IA. Similarly, ITS2 sequences of different AG3 and AG4 subgroups are clustered within their respective clade, whereas the outgroup *T. calospora* shows distinct architecture, providing strong evidence in favor of the correct methods used for genome assemblies. Intriguingly, the ITS2 sequences of AG8 subgroup shows remarkable differences, in which sequence of tester strain (i.e., AG-8-A68), previously published genome sequence (i.e., AG8-01) and from the reported genome of this study (i.e., AG8-Rh89/T) are clustered across different clade of the phylogenetic tree.

One of the important proteins known to be strongly associated with fungal evolution and virulence is the penta-functional AROM sequence, with characteristic five domains (64). Here,

265 we characterized the AROM protein sequences in the predicted proteome of all given assemblies
266 (Figure S3). We observed at least one penta-functional AROM sequence in each of the
267 assemblies, in which sequence(s) are present in either complete or partial form. Interestingly,
268 AG3-1A1 has two complete penta-functional AROM protein sequences, a characteristic not
269 observed in any other AG. In AG5, two partial AROM sequences are observed that together
270 completed all five domains observed in the complete penta-functional AROM sequence (65).
271 Although, all assemblies are found to have contiguous AROM protein sequences, the partial
272 AROM sequences in AG5 may represent a fragmented region of the genome assembly and,
273 therefore, warrants further experimental investigations and genome assembly improvements.

274 **Genome-wide orthologous protein clustering and functional analysis**

275 Intron/exon and transcript boundaries were identified using the maker pipeline (see materials and
276 methods), which predicted 7,394 to 10,958 protein coding transcripts per genome (excluding *T.*
277 *calospora*, Figure S4) in which AG3-1A1 genome has the highest number of transcripts. Next,
278 using OrthoMCL, the translated protein sequences in all genomes were clustered into the
279 orthologous groups, where each cluster of proteins represented a set of similar sequences likely
280 to represent a protein family. The similarities among the given isolates were enumerated by
281 measuring proteins shared by different proteomes in the same orthoMCL clusters (Figure 2A).
282 As expected, this analysis clearly outgroup *T. calospora*, indicating that it has a different protein
283 family composition than *R. solani* isolates. Although, AG1 and AG4 subgroups, AG3-1A1 and
284 AG3-1AP shows expected similarities and share similar clustering profiles, AG3-PT and AG5
285 shows a divergent profile of protein families with respect to the other AGs under study.
286 Nevertheless, a large set of orthoMCL clusters share proteins from all/most of the *R. solani*
287 isolates which further indicates inherent similarities as well as unique attributes across these

pathologically diverse groups of fungi. For instance, more than 1,400 orthoMCL clusters are composed of proteins belonging to only two AGs, whereas >1,500 clusters are composed of proteins from all 13 *R. solani* isolates and *T. calospora* (Figure 2B). It is expected that these conserved clusters are composed of proteins from core gene families with essential functions, whereas other clusters may host proteins with unique AG-specific roles (Figure 2C). The analysis reveals that AG1-1C, AG2-2IIIB, AG5, AG6-10EEA and AG8 are composed of large number of unique proteins (>1,000 proteins), whereas AG3-1A1 has the highest number of core and auxiliary proteins. The pair-wise comparison of the number of clusters shared by any two AGs highlighted that AG3-1AP shares the highest number of orthoMCL clusters with AG3-1A1, a sector derived hypo-virulent isolate of AG3-1AP (Figure 2D) (66). In fact, AG3-1A1 proteins shares large number of clusters with few other AG subgroups too, including AG1-1C, AG6-10EEA, AG2-2IIIB and AG4-R118.

To investigate the functional composition of proteins using orthologous groups information, we performed InterPro domain family analysis of proteomes from each AG (Figure S5). Interestingly, the core proteome of most AGs is composed of ~2,000 InterPro domain families, whereas the unique proteome per AG ranged between 101 (for AG3-PT) to 628 (for AG3-1A1). Wherein, the most common protein family that made the unique proteome of *R. solani* subgroups is “Cytochrome P450”, which is essential for fungal adaptations to diverse ecological niches (67) (Figure 3). Similarly, proteins with WD40 repeats are found to be the most common set of the unique proteome in most AGs. In addition, few of the AG subgroups are found to be enriched with a protein family that is significantly associated with its unique proteome only, possibly being involved in the survival of that AG in respective hosts. For instance, the AG1-IB unique proteome is enriched with “NADH: Flavin Oxidoreductase/ NADH

oxidase (N-terminal)", similarly AG3-1A1 is enriched with "ABC transporter-like" and "Aminoacyl-tRNA synthetase (class-II)" InterPro domains. Whereas AG3-PT is found to be uniquely enriched with "Ribosomal protein S4/S9" and AG3-1A1 is uniquely enriched with "Multicopper oxidase (Type 2)" and "Patatin like phospholipase domain".

The predicted secretome and effector proteins

To facilitate host colonization, plant pathogens secrete proteins to host compartments that modulate morphological changes in the host system and establish fungal infection (68–70). Therefore, we identified the comprehensive set of secreted proteins from all *R. solani* and *T. calospora* genomes. Figure 4A shows the number of secreted proteins identified in each of the given genomes, wherein AG1-IC, AG3-1A1, AG6-10EEA and AG2-2IIIB contains a large number of proteins in the predicted secretome (Supplementary file, sheet 1-2). However, AG1,1C, AG2-2IIIB and AG8 contains a comparatively larger number of isolate-specific secreted proteins (i.e., secreted proteins in the unique proteome), while AG3-1AP, AG3-1A1 and AG3-PT contains comparatively lower number of secreted proteins. Interestingly, InterPro domain analysis of the secreted proteins suggests that the most enriched protein domain in the predicted secretome is "cellulose binding domain – fungal" (Figure 4B) which is essential for the fungal patho-system for the degradation of cellulose and xylans (71). In addition, the secretomes are also enriched with proteins containing "Glycoside Hydrolase Family 61", "Pectate Lyase" and "multi-copper oxidase family" domains. Most of these protein components include enzymes essential for degradation of the plant host cell wall and breaking down the first line of host defense. We observed that certain families of protein domains are found to be enriched within a few AGs only. For instance, "aspartic peptidase family A1" domain containing proteins, involved in diverse fungal metabolic processes, are mainly enriched in AG2-2IIIB

isolate, similarly "lysine-specific metallo-endopeptidase" are enriched in AG3-1AP, AG5 and AG8. The AG4-R118 secretome is significantly enriched with proteins belonging to "Glycoside Hydrolase Family 28" and "Peptidase S8 propeptide-proteinase inhibitor I9" domains, whereas AG4-RS23 secretome is composed of "NodB homology" and "alpha/beta hydrolase fold-1" domains. Taken together, the analysis indicates that each of the given AG secretome is significantly enriched with a unique set of protein families that possibly allows the fungal patho-system to perform a variety of biological functions in different host systems and patho-systems.

Next, to identify the unique and conserved attributes associated with *R solani*, we performed a comparative analysis of the secretome with 14 other fungi (excluding *T. calospora*), which represented the major taxonomic, pathogenic, ecological, and commercially important (edible fungi) groups within the Division Basidiomycota. (Table S4). We hypothesized that small set of functionally important proteins, e.g., secreted proteins, in *R. solani* may have the unique attributes not observed within the other basidiomycetes. Therefore, we predicted the secretome and analyzed the InterPro domains in the secreted proteins of 14 different basidiomycetes and compared with the secretome of *R. solani* AGs. We observed that the number of secreted proteins predicted in *R solani* AGs are not significantly different to the number of secreted proteins in other Basidiomycetes ($p=0.0629$; Figure 4C). However, the InterPro domains enriched in the secretome of *R. solani* AGs and other basidiomycetes are found to be significantly different. We observed that only a limited number of InterPro terms are shared between *R. solani* AGs and other basidiomycetes, and *R. solani* AGs are functionally closer to each other than other basidiomycetes (Figure 4D), which suggests that *R. solani* secretome have a unique domain profile, which are primarily different from other Basidiomycetes. Overall, we found 565 InterPro terms in the secretome of *R. solani*, whereas in other basidiomycetes

(including *T. calospora*), secretomes are enriched with 620 terms in which 283 InterPro terms are common across both the group of species. We observed 282 InterPro terms (50%) uniquely associated with *R. solani*, not observed in the secretome of other basidiomycetes, whereas 337 InterPro terms are only observed in the secretome of other basidiomycetes. The analysis of *R. solani* specific 282 InterPro terms includes several protein domains belonging to diverse functional significance, e.g., "Aspartic peptidase A1 family", "Cysteine rich secretory protein related" and "Polyscaccaride lyase 8" domains. Among the domains commonly enriched across both *R. solani* isolates and other basidiomycetes, we calculated the fold change of difference of domain occurrence in their secretome and enumerated the proteins domains with significant differences across *R. solani* and other basidiomycetes (Supplementary file, sheet 1-2). Our analysis suggests, high differences in domains frequency wherein, protein with domains like "Pectate lyase", "Serine amino-peptidase" and "Lysine-specific metallo-endopeptidase" are significantly enriched in *R. solani* secretome. Similarly, proteins with "Hydrophobin" and "Zinc finger ring-type" domains are majorly enriched in other basidiomycetes. We believe that such large number of unique functional domains in the secreted proteome of *R. solani* may be functionally relevant that allows these fungi to survive in diverse array of conditions, and thus should further be investigated experimentally for understanding their role in survival.

Although these plant pathogenic fungi secrete a large number of proteins, only a small proportion of these proteins have been implicated to be effectively associated with fungal-plant interactions, i.e. effector proteins (68–70). Effector proteins can strongly inhibit the activity of host cellular proteases and allow pathogenic fungi to evade host defense mechanisms. Fungal effector proteins are not known for having a conserved family of domains, these proteins typically are of small length (300-400 amino acids) and higher cysteine content (55, 69, 72). Our

380 analysis reveals 75-134 effector proteins predicted in *R. solani* genomes, whereas *T. calospora*
381 contains 136 effector proteins (Figure 5A; supplementary file S1-S7).

382 Isolates from AG1-IC contains the highest number of effector proteins (*n*=134), whereas
383 isolate from AG3-PT contains a small number of effectors (*n*=75). Nevertheless, all the isolates
384 are composed of approximately 100 effector proteins which contain a similar proportion of
385 cysteine residues in the predicted effector proteins (Figure 5B). Next, we investigated the
386 topmost enriched domains among all *R. solani* effector proteins in which "Pectate lyase" is found
387 to be the most enriched effector protein, followed by "thaumatin family" of domain containing
388 proteins (Figure 5C).

389 In comparison, the analysis of effector proteins in other basidiomycetes suggests that all
390 other basidiomycetes are enriched with similar number of effector proteins (p-value = 0.14;
391 Figure 5C-D; supplementary file; sheet 3-4). Wherein, the effector proteins in *R solani* AGs
392 includes the proteins belonging to 237 InterPro terms, whereas the effector proteins of other
393 basidiomycetes (including *T. calospora*) include proteins enriched with 119 terms. We found 173
394 terms (72%) are uniquely associated with *R solani* AGs, in which most abundant terms includes
395 IPR001283 (Cystine rich secretory protein related). These unique effectors may play the
396 deciding roles on host recognition and in virulence of necrotrophic *Rhizoctonia* pathogens (73,
397 74) . Moreover, we also observed 55 InterPro terms not observed with *R solani* effector proteins,
398 including Zinc Finger and LysM domain. We also found 64 InterPro terms commonly enriched
399 by both the groups of effector proteins, in which "Pectate lyase" and "Glycoside hydrolase
400 family 28" are mainly associated with *R. solani* AG subgroups effector proteins, whereas
401 "Hydrophobin" is mainly associated with other basidiomycetes. The complete list of secretome,

effector proteins, the InterPro domains and associated information are available in supplementary file.

Carbohydrate-active enzymes

CAZymes are essential for degradation of host plant cells and fungal colonization in the host, and are, thus important for fungal bioactivity (75, 76). Using CAZy (Carbohydrate Active Enzyme database) (77), which contains the classified information of enzymes involved in complex carbohydrate metabolism, we annotated and compared the distribution of CAZymes in all *R. solani* isolates. Overall, *R. solani* isolates are composed of 383-595 high confidence CAZymes, with AG3-1A1 having the largest number of CAZymes (Figure 6A). These predicted CAZymes in *R solani* AGs are mainly distributed across 177 CAZyme families that can be broadly classified into six major classes of enzymes, i.e., Glycoside Hydrolase (GH), Polysaccharide Lyase (PL), Carbohydrate Esterase (CE), Carbohydrate-binding modules (CBM) and redox enzymes with Auxiliary Activities (AA). Our analysis reveals that GH forms the major class of CAZymes in all fungal species, including *T. calospora* (Figure S6 and S7), which hydrolyzes the glycosidic bonds between carbohydrate and non-carbohydrate moieties or between two or more carbohydrate moieties (78). Whereas CBM forms the least abundant class of enzymes enriched in the proteomes of the given isolates. Despite the differences, we observed similar distribution of enzyme count in each class of CAZyme across all the given isolates.

We found that among the predicted 177 families, only 34 families are abundant (with total enzyme count > 50 proteins; Figure 6B) across all the given isolates, i.e., *Rhizoctonia* species and *T. calospora*. These 36 families have a distinct abundance profile in each AG, for instance, protein from GH7 family is highly abundant in *T. calospora* as compared to the *R solani* isolates. Similarly, proteins belonging to PL1_4 are not observed in AG4-R118 and *T. calospora*. We

have divided these 34 families into three different groups, with respect to their abundance profile in *R. solani* isolates. The Group-1 contains CAZymes belonging to GH28, AA9, PL3_2 and AA3_2 families and form the highly abundant families (total enzyme count >200 proteins) of enzymes in *R Solani* AGs. Similarly, Group-2 contains 11 CAZyme families with enzymes moderately abundant in *R Solani* AGs. Whereas Group-3 contains 19 families with sparsely abundant CAZymes. We observed that in all the three clusters, AG3-1A1 contains the highest number of CAZymes for most the 34 families, and significantly enriched with all the members of Group-1 families. In fact, the clustering analysis highlights the similar profiles of AG3-1A1 and AG2-2IIIB, mainly due to similar distribution of proteins belonging to GH28, AA9, AA3_2 and GH7. In Group-1, although GH28 containing enzymes are abundant in most of the *R. solani* isolates, AG8 contains limited number of enzymes belonging to this family. Similarly, AA9 and PL3_2 families of enzymes are abundant only in 50% of the isolates, and thus may be relevant for a unique set of functions associated with the respective isolates. In Group-2, however, we observed similar distribution of abundance profile across all the isolates, except *T. calospora*, which indicates their probable role in *R. solani* specific function. For examples, CAZymes belonging to AA5_1, GH18 and PL4_1 are enriched in most of the *R. solani* isolates, but not in *T. calospora*. The conserved distribution of CAZymes families in the diverse proteomes of different *R. solani* isolates signifies their essential role in fungal activity. On the other hand, Group-3 CAZymes provide unique and distinct profile to each AG with a limited number of families showing similar abundance profile. Wherein, *T. calospora* is found to be distinctly abundant in CAZymes belonging to GH5_5, not observed with *R. solani* isolates. These results strongly suggested that *R. solani* isolates share a large proportion of carbohydrate degrading enzymes, in which an isolate-specific CAZyme profile can also be observed (mainly from

Group-3). To confirm, if the abundance profile is strictly associated with *R. solani* isolates, we performed the comparative analysis with abundance profile of 14 other basidiomycetes. The analysis clearly reveals the distinct CAZymes profile than other Basidiomycetes, in which *R. solani* isolates can be phylogenetically grouped into a different cluster (Figure S8). The analysis highlights the families that uniquely abundant in *R. solani* isolates than other basidiomycetes, e.g., GH28, PL3_2, AA5_1, CE4, GH10, GH62, PL4_1, CE8, PL1_7, PL1_4 and AA7, and as expected, most of these families belong to Group-1 and Group-2 of the previous analysis. Among these families, we observed that PL3_2, GH62 and CE8 families of proteins are distinctly expressed in *R. solani* isolates. In addition, AG3-1A1 is exceptionally abundant in AA9 and GH28, not observed with any other basidiomycetes under investigation. In contrast, AA3_2 (Group-1) is abundant in most of the basidiomycetes, including *R. solani*. In summary, we have shown that members of CAZymes families belonging to Group-1 and Group-2 are abundant in *R. solani* isolates and may also provide them a unique attribute (or functions) not observed with the other basidiomycetes.

RsolaniDB: a *Rhizoctonia solani* pangenome database and its applications

RDB is a large-scale, integrative repository for hosting the *R. solani* pangenome project with emphasis on supporting data mining and analysis, wherein the genomes and their components can be accessed under three different categories, viz. genomic, ortholog and functional assignment.

Genomes: The genomic content includes draft genome sequences of *R. solani* isolates in FASTA format along with the gene level annotation in GFF3 format. The annotation includes prediction of gene boundaries with introns and exons, as well as their locations on contigs or scaffolds. It also includes the predicted transcribed cDNA sequences and translated protein sequences. This

information is vital for those users looking for reference genomes and their annotated components for mapping RNAseq reads. The draft genomes and their annotation can also be downloaded and used for downstream local analysis, e.g., variants calling, SNP, eQTLs analysis and other similar genomic analyses with different bioinformatics methods.

Orthologs: Using the orthoMCL clustering on the proteomes of 18 *R. solani* (including previously published genome assemblies), protein sequences were compared and clustered into groups of similar sequences. The sequences not part of any of the clusters, i.e., singletons, and unique to respective isolates were categorized as "unique". Whereas the rest of the proteome was categorized either into "core" or "auxillary" groups of orthoMCL clusters. RDB allows users to retrieve this information for each protein entry and also allows users to retrieve the protein ID of other members of its ortholog cluster family, if any.

Functional assignment: This category includes the predicted InterPro protein domains associated with each of the protein entries. RDB also includes GO information associated with each protein, along with PANTHER pathway terms. This information helps in assigning the functional description for each protein entry in the database.

The database is organized to include one unique RDB ID (or entry) for each gene structure, with all of the above associated information. The RDB ID allows users to search the genomic coordinates (intron/exon boundaries) with IGV visualization, sequences and its functional annotation, for each gene in each *R. solani* isolate. All of this information can be retrieved from the database via the "text-based" or "keywords-based" search in an AG-specific manner or from the entire database. Users can also perform blast searches of their own nucleotide or protein sequences to the entire database or can target a given AG. Moreover, users can retrieve the set of sequences in FASTA format, for a given list of RDB IDs. One of the

494 important and unique features of RsolaniDB tools allows users to perform functional or gene-set
495 enrichment analysis of given RDB IDs, e.g., Gene Ontology or pathway analysis. This feature is
496 especially useful for analyzing differentially expressed genes after RNAseq data analysis, as it
497 provides the statistical significance (as *p*-values) of different GO/pathway terms enriched in a
498 given set of differentially expressed genes. As far as we know, this feature is unique to RDB
499 with respect to any other existing *Rhizoctonia* resources. However, it requires the user to use
500 reference genome sequences and the annotation file from RDB database for subjecting into
501 RNAseq data analysis pipeline. As an additional resource, RDB also incorporated previously
502 published (16, 18, 20, 79–81) genome and transcriptome level information in a single platform
503 with an RDB ID format. The database is publicly available to the scientific community,
504 accessible at http://rsolanidb.kaust.edu.sa/RhDB/index.html.

505 **Discussion**

506 *Rhizoctonia solani* is considered as one of the most destructive and a diverse group of soil-borne
507 plant pathogens causing various diseases on a wide range of economically important crops. It is
508 classified into 13 AGs with distinctive pathogenic host range and responsiveness to disease
509 control measures. For example, AG1, AG2-2IIIB, and AG4 cause diseases mostly on cool-
510 season turfgrasses, whereas AG2-2LP, causing large patch disease, is predominantly seen on
511 warm season turfgrasses (82, 83). Isolates from different AGs also vary in sensitivity to
512 fungicides and no single fungicide is effective against all AGs (84). For example, AG5 isolates
513 are moderately sensitive to pencycuron, while other AGs are highly sensitive to this fungicide
514 (85). Our ability to control this pathogen is hampered by a lack of accurate molecular
515 identification of AGs and its subgroups, and poor understanding of the genetic variation among

them. This genetic variation results in differing sensitivity to control measures, as well as the pathogenic and ecological diversity in the population structures of the *R. solani* complex. One of the primary reasons for this limited understanding of the *R. solani* complex is the lack of genetic studies representative of its heterozygous and diverse AGs and sub-groups (13). Until now, draft genome assemblies belonging to only four of the 13 AGs had been reported; viz. AG1-IA (16), AG1-IB (17), AG2-2IIIB (13), AG3-Rhs1AP (18), AG3-PT isolate Ben-3 (19) and AG8 (20). Here we expanded the scope of genetic analysis of the *R. solani* complex by performing comprehensive genome sequencing, assembly, annotation and comparative analysis of 12 *R. solani* isolates. This enabled us to perform pangenome analysis of *R. solani* to 7 AGs (AG1, AG2, AG3, AG4, AG5, AG6, AG8), selected additional sub-groups (AG1-IC, AG3-TB), and a hypovirulent isolate (AG3-1A1). Although heterokarotic and diploid nature of *Rhizoctonia* species are expected to cause the genome assembly challenges (13), in our analysis we observed of a large number of inter-groups syntenic regions and ITS2-based similarities which highlights the high similarities among the given 13 *R. solani* isolates (including AG3-PT). The recognition of conserved ITS2 sequences along with large syntenic regions despite the physiological and taxonomic differences in the given isolates suggests the essentially conserved regions and high quality of the draft genome sequences generated in this study.

Subsequently, to deduce the similarities as well as unique features in the given set of predicted proteomes, we performed a series of comparative analyses that indicated the expected heterogeneity among *R. solani* subgroups with the orchid mycorrhizal fungus *T. calospora* as an outlier. For example, both AG5 and AG2-2IIIB included a large set of unique proteomes as well as secretomes, enriched with InterPro families of proteins that are abundant in these two AGs. Additionally, the proteome of *R. solani* isolates are uniquely and highly enriched with proteins

539 with “pectate lyase” domains, as compared to the other basidiomycetes. Another finding of
540 potential significance is that the highest number of orthoMCL clusters were shared between
541 AG3-1A1 and AG3-1AP, both isolates belonging to the AG3-PT subgroup. Isolate AG3-1A1 is
542 the sector-derived, hypovirulent isolate of the more virulent isolate, AG3-1AP. Intriguingly,
543 AG3-1A1 has been demonstrated to be a successful biocontrol agent of isolate AG3-1AP in the
544 field (86). Competitive niche exclusion is a demonstrated mechanism for biocontrol where the
545 biocontrol agent has a significant overlap in resource utilization with the pathogen and
546 outcompetes the pathogen for these necessary resources (87). A high degree of overlap in gene
547 function is consistent with the mechanism of biocontrol of AG3-1AP in the field by AG3-1A1
548 through competitive niche exclusion.
549 The sector-derived, hypovirulent isolate AG3-1A1 however differed from the progenitor isolate
550 AG3-1AP, as well as the other *R. solani* isolates analyzed, in AROM sequences. AROM
551 sequences are known for their conserved profile across fungal species and encode the penta-
552 functional AROM polypeptide that catalyzes five consecutive enzymatic reactions in the
553 prechorismate steps of the shikimate pathway; leading to biosynthesis of the aromatic amino
554 acids tryptophan, tyrosine, and phenylalanine(65). The isolate AG3-1A1 contained two complete
555 penta-functional AROM protein sequences while other isolates contained only one complete
556 sequence or partial AROM sequences. Sectoring as a means of phenotypic plasticity in fungi
557 may take place by genetic mutations, rearrangement of heterokaryotic nuclei, conversion from
558 heterokaryotic to homokaryotic mycelium, exchange of cytoplasmic factors, etc., resulting in
559 changes in morphology, virulence, mating type, sporulation, and ecological adaptations (88). It is
560 possible that the genetic event that led to duplication of the AROM sequences in AG3-1A1 led to
561 hypovirulence. Phenylacetic acid (PAA) has been demonstrated to be a virulence factor in the

progenitor isolate, AG3-1AP, and that downregulation of the shikimate pathway occurs in AG3-1A1; resulting in a reduction in production of PAA by AG3-1A1(89). Moreover, possibilities exist that one of the two *arom* genes in AG3-1A1 remains inactive due to methylation, or that the gene duplication is an attempt to compensate for the suppressed shikimate pathway as documented in *Aspergillus nidulans* (65). However, further investigation is necessary to determine if any of those hypotheses is true.

Secretome analysis also revealed several interesting findings that provided unique characteristics to each *R. solani* isolate, e.g., secretome of AG1-1B and AG3-T5 are uniquely and significantly enriched with three different multi-copper oxidases (type 1/2/3), both of which are known to cause foliar diseases. Nevertheless, despite the differences, most of the secretome have similar composition in their significantly enriched protein domains, which mainly includes "Cellulose-binding domain fungal", "Glycoside hydrolase family 61" and "Pectate lyase". However, the composition is significantly different with respect to the other basidiomycetes and large number of reported protein families are uniquely associated with multiple *R. solani* isolates. We observed similar finding for the effector proteins, wherein protein containing “Cysteine rich secretory proteins”, “Pectate lyase” and “Thaumatin” are distinctly abundant in *R. solani* isolates, whereas “Hydrophobin” is only abundant in other basidiomycetes. Similarly, the CAZyme analysis highlighted several unique attributes associated with each *R. solani* species especially AG3-1A1 by possessing the CBM1 family of proteins which are linked with degradation of insoluble polysaccharides (90). It was observed that several families of these CAZymes were not present in *T. calospora* which is a symbiotic mycorrhizal fungus and other basidiomycetes, e.g. GH28, PL3_2, AA5_1 and GH10 (91). Overall, data presented in this study are consistent with the hypothesis that AG and sub-groups of *Rhizoctonia* species are highly

585 heterogeneous, each with unique functional genomic properties, while being conserved in their
586 functional regions with respective other groups. However, the unique secretomes, effector and
587 similarly CAZymes profiles of *R. solani* over other basidiomycetes may reflect the ecological
588 and host adaptation strategies, as well as the necrotrophic lifestyle of the former, and call for
589 future research in respective areas to better understand the biology and pathology of the species.
590 To further propel research with *R. solani* we present our data as the web-resource
591 RsolaniDB (RDB). This web-resource includes detailed information on each *R. solani* isolate,
592 such as the genome properties, predicted transcript/protein sequences, predicted function, and
593 protein orthologues among other AG sub-groups, along with tools for Gene Ontology (GO) and
594 pathway enrichment analysis, orthologs, sequence analysis and IGV visualization of gene
595 models. Also, by adding the previously published genome assemblies and their features,
596 RsolaniDB stands as the universal platform for accessing *R. solani* resources with single
597 identifier format. Since none of the existing Rhizoctonia specific databases host such a large
598 repertoire of genome assemblies and accessory web-tools for functional enrichment analysis of
599 gene set, e.g., differentially expressed genes, RsolaniDB stands as a valuable resource for
600 formulating new hypotheses and understanding the unique or conserved patho-system of *R.*
601 *solani* AGs and subgroups. The associated gene-set enrichment analysis tool further sets
602 RsolaniDB apart from the existing fungal databases which does not allow the gene enrichment
603 analysis.
604 Finally, since, each of the *R. solani* AGs or subgroups is characterized by a unique
605 heterogeneous profile, we strongly believe that the presented genome assemblies, annotation and
606 comparative analysis will facilitate mycologists and plant pathologists generating a greater
607 understanding of its biology and ecology, and in developing as well as improving the existing *R.*

608 *solani* disease management projects, including drug target discovery and design of future
609 diagnostic tools for rapid discrimination of *R. solani* AGs under indoor and outdoor farming
610 environments.

611 **Data availability**

612 All data is publicly available as the error corrected, processed fastq files at European Nucleotide
613 Archive (ENA) at EMBL-EBI under primary accession ID PRJEB39881 (secondary accession:
614 ERP123449) (92, 93). Genome assemblies and corresponding annotations are available at
615 RsolaniDB database (http://rsolanidb.kaust.edu.sa/RhDB/index.html)

616 **Funding**

617 This project was funded by USDA-ARS fund [Agreement #-58-8042-8-067-F USDA-KAUST
618 project] to DKL and a KAUST faculty baseline fund [BAS/1/1020-01-01] to AP.

619 **Acknowledgements**

620 The authors thank the members of the Bioscience Core Laboratory (BCL) in KAUST for
621 producing the raw DNA and RNA sequence datasets and Adnan (Ed) Ismaiel (USDA-ARS,
622 SASL, for DNA extraction and fungal culture maintenance). We also thank Drs. Ian Misner and
623 Nadim Alkharouf (Towson University, Towson, MD.) for helping during the initial setting-up of
624 the project.

625 **Author contributions**

626 A.K., D.K.L. and A.P. conceived the study, interpreted the results and wrote the manuscript;
627 A.K. performed the bioinformatics analysis and developed the computational pipelines and the
628 database; A.R., S.M. and M.N. conducted the molecular experiments, library preparation and

629 sequencing; D.P.R. collected and stored the materials and edited the manuscript; A.P. and D.K.L.

630 supervised the overall project.

631 **References**

632 1. Yang,G. and Li,C. (2012) General Description of Rhizoctonia Species Complex INTECH
633 Open Access Publisher.
634 2. Amaradasa,B.S., Horvath,B.J., Lakshman,D.K. and Warnke,S.E. (2013) DNA fingerprinting
635 and anastomosis grouping reveal similar genetic diversity in rhizoctonia species infecting
636 turfgrasses in the transition zone of USA. *Mycologia*, **105**, 1190–1201.
637 3. Raaijmakers,J.M., Paulitz,T.C., Steinberg,C., Alabouvette,C. and Moënne-Loccoz,Y. (2009)
638 The rhizosphere: A playground and battlefield for soilborne pathogens and beneficial
639 microorganisms. *Plant Soil*, **321**, 341–361.
640 4. Gónzalez,D., Rodriguez-Carres,M., Boekhout,T., Stalpers,J., Kuramae,E.E., Nakatani,A.K.,
641 Vilgalys,R. and Cubeta,M.A. (2016) Phylogenetic relationships of Rhizoctonia fungi within
642 the Cantharellales. *Fungal Biol.*, **120**, 603–619.
643 5. Keijer,J., Korsman,M.G., Dullemans,A.M., Houterman,P.M., De Bree,J. and Van
644 Silfhout,C.H. (1997) In vitro analysis of host plant specificity in Rhizoctonia solani. *Plant*
645 *Pathol.*, **46**, 659–669.
646 6. Foley,R.C., Gleason,C.A., Anderson,J.P., Hamann,T. and Singh,K.B. (2013) Genetic and
647 Genomic Analysis of Rhizoctonia solani Interactions with Arabidopsis; Evidence of
648 Resistance Mediated through NADPH Oxidases. *PLoS One*, **8**, e56814.
649 7. Gonzalez,D., Carling,D.E., Kuninaga,S., Vilgalys,R. and Cubeta,M.A. (2001) Ribosomal
650 DNA systematics of Ceratobasidium and Thanatephorus with Rhizoctonia anamorphs .
651 *Mycologia*, **93**, 1138–1150.
652 8. Hane,J.K., Anderson,J.P., Williams,A.H., Sperschneider,J. and Singh,K.B. (2014) Genome
653 sequencing and comparative genomics of the broad host-range pathogen Rhizoctonia solani
654 AG8. *PLoS Genet.*, **10**, e1004281.
655 9. Hossain,M.K., Tze,O.S., Nadarajah,K., Jena,K., Bhuiyan,M.A.R. and Ratnam,W. (2014)
656 Identification and validation of sheath blight resistance in rice (Oryza sativa L.) cultivars
657 against Rhizoctonia solani. *Can. J. Plant Pathol.*, **36**, 482–490.
658 10. Copley,T., Bayen,S. and Jabaji,S. (2017) Biochar Amendment Modifies Expression of

659 Soybean and Rhizoctonia solani Genes Leading to Increased Severity of Rhizoctonia Foliar
660 Blight. *Front. Plant Sci.*, **8**, 221.
661 11. Anderson,J.P., Hane,J.K., Stoll,T., Pain,N., Hastie,M.L., Kaur,P., Hoogland,C., Gorman,J.J.
662 and Singh,K.B. (2016) Proteomic analysis of rhizoctonia solani identifies infection-specific,
663 redox associated proteins and insight into adaptation to different plant hosts. *Mol. Cell.*
664 *Proteomics*, **15**, 1188–1203.
665 12. Lakshman,D.K., Roberts,D.P., Garrett,W.M., Natarajan,S.S., Darwish,O., Alkharouf,N.,
666 Pain,A., Khan,F., Jambhulkar,P.P. and Mitra,A. (2016) Proteomic Investigation of
667 Rhizoctonia solani AG 4 Identifies Secretome and Mycelial Proteins with Roles in Plant
668 Cell Wall Degradation and Virulence. *J. Agric. Food Chem.*, **64**, 3101–3110.
669 13. Wibberg,D., Andersson,L., Tzelepis,G., Rupp,O., Blom,J., Jelonek,L., Pühler,A.,
670 Fogelqvist,J., Varrelmann,M., Schlüter,A., *et al.* (2016) Genome analysis of the sugar beet
671 pathogen Rhizoctonia solani AG2-2IIIB revealed high numbers in secreted proteins and cell
672 wall degrading enzymes. *BMC Genomics*, **17**, 245.
673 14. Zhang,J., Chen,L., Fu,C., Wang,L., Liu,H., Cheng,Y., Li,S., Deng,Q., Wang,S., Zhu,J., *et al.*
674 (2017) Comparative transcriptome analyses of gene expression changes triggered by
675 Rhizoctonia solani AG1 IA infection in resistant and susceptible rice varieties. *Front. Plant*
676 *Sci.*, **8**, 1422.
677 15. Shu,C., Zhao,M., Anderson,J.P., Garg,G., Singh,K.B., Zheng,W., Wang,C., Yang,M. and
678 Zhou,E. (2019) Transcriptome analysis reveals molecular mechanisms of sclerotial
679 development in the rice sheath blight pathogen Rhizoctonia solani AG1-IA. *Funct. Integr.*
680 *Genomics*, **19**, 743–758.
681 16. Nadarajah,K., Razali,N.M., Cheah,B.H., Sahruna,N.S., Ismail,I., Tathode,M. and Bankar,K.
682 (2017) Draft genome sequence of Rhizoctonia solani anastomosis group 1 subgroup 1A
683 strain 1802/KB isolated from rice. *Genome Announc.*, **5**.
684 17. Wibberg,D., Rupp,O., Blom,J., Jelonek,L., Kröber,M., Verwaaijen,B., Goesmann,A.,
685 Albaum,S., Grosch,R., Pühler,A., *et al.* (2015) Development of a Rhizoctonia solani AG1-
686 IB Specific Gene Model Enables Comparative Genome Analyses between Phytopathogenic
687 R. solani AG1-IA, AG1-IB, AG3 and AG8 Isolates. *PLoS One*, **10**.
688 18. Cubeta,M.A., Thomas,E., Dean,R.A., Jabaji,S., Neate,S.M., Tavantzis,S., Toda,T.,
689 Vilgalys,R., Bharathan,N., Fedorova-Abrams,N., *et al.* (2014) Draft Genome Sequence of

690 the Plant-Pathogenic Soil Fungus Rhizoctonia solani Anastomosis Group 3 Strain Rhs1AP.
691 *Genome Announc.*, **2**.
692 19. Wibberg,D., Genzel,F., Verwaaijen,B., Blom,J., Rupp,O., Goesmann,A., Zrenner,R.,
693 Grosch,R., Pühler,A. and Schlüter,A. (2017) Draft genome sequence of the potato pathogen
694 Rhizoctonia solani AG3-PT isolate Ben3. *Arch. Microbiol.*, **199**, 1065–1068.
695 20. Hane,J.K., Anderson,J.P., Williams,A.H., Sperschneider,J. and Singh,K.B. (2014) Genome
696 Sequencing and Comparative Genomics of the Broad Host-Range Pathogen Rhizoctonia
697 solani AG8. *PLoS Genet.*, **10**.
698 21. Bills,G.F., Singleton,L.L., Mihail,J.D. and Rush,C.M. (1993) Methods for Research on
699 Soilborne Phytopathogenic Fungi The American Phytopathological Society,.
700 22. Carlson,J.E., Tulsieram,L.K., Glaubitz,J.C., Luk,V.W.K., Kauffeldt,C. and Rutledge,R.
701 (1991) Segregation of random amplified DNA markers in F1 progeny of conifers. *Theor.*
702 *Appl. Genet.*, 10.1007/BF00226251.
703 23. Sayers,E.W., Beck,J., Brister,J.R., Bolton,E.E., Canese,K., Comeau,D.C., Funk,K., Ketter,A.,
704 Kim,S., Kimchi,A., *et al.* (2020) Database resources of the National Center for
705 Biotechnology Information. *Nucleic Acids Res.*, 10.1093/nar/gkz899.
706 24. Bolger,A.M., Lohse,M. and Usadel,B. (2014) Trimmomatic: A flexible trimmer for Illumina
707 sequence data. *Bioinformatics*, **30**, 2114–2120.
708 25. Simon Andrews (2020) Babraham Bioinformatics - FastQC A Quality Control tool for High
709 Throughput Sequence Data. *Soil*, **5**, 47–81.
710 26. Marçais,G. and Kingsford,C. (2011) A fast, lock-free approach for efficient parallel counting
711 of occurrences of k-mers. *Bioinformatics*, **27**, 764–770.
712 27. Grabherr,M.G., Haas,B.J., Yassour,M., Levin,J.Z., Thompson,D.A., Amit,I., Adiconis,X.,
713 Fan,L., Raychowdhury,R., Zeng,Q., *et al.* (2011) Full-length transcriptome assembly from
714 RNA-Seq data without a reference genome. *Nat. Biotechnol.*, **29**, 644–652.
715 28. Bankevich,A., Nurk,S., Antipov,D., Gurevich,A.A., Dvorkin,M., Kulikov,A.S., Lesin,V.M.,
716 Nikolenko,S.I., Pham,S., Prjibelski,A.D., *et al.* (2012) SPAdes: A new genome assembly
717 algorithm and its applications to single-cell sequencing. *J. Comput. Biol.*, **19**, 455–477.
718 29. Gurevich,A., Saveliev,V., Vyahhi,N. and Tesler,G. (2013) QUAST: Quality assessment tool
719 for genome assemblies. *Bioinformatics*, **29**, 1072–1075.
720 30. Boetzer,M., Henkel,C. V., Jansen,H.J., Butler,D. and Pirovano,W. (2011) Scaffolding pre-

721 assembled contigs using SSPACE. *Bioinformatics*, 10.1093/bioinformatics/btq683.
722 31. Luo,R., Liu,B., Xie,Y., Li,Z., Huang,W., Yuan,J., He,G., Chen,Y., Pan,Q., Liu,Y., *et al.*
723 (2012) SOAPdenovo2: An empirically improved memory-efficient short-read de novo
724 assembler. *Gigascience*, **1**, 18.
725 32. Song,L., Shankar,D.S. and Florea,L. (2016) Rascaf: Improving Genome Assembly with RNA
726 Sequencing Data. *Plant Genome*, **9**, plantgenome2016.03.0027.
727 33. Seppey,M., Manni,M. and Zdobnov,E.M. (2019) BUSCO: Assessing genome assembly and
728 annotation completeness. In *Methods in Molecular Biology*. Humana Press Inc., Vol. 1962,
729 pp. 227–245.
730 34. Bengtsson-Palme,J., Ryberg,M., Hartmann,M., Branco,S., Wang,Z., Godhe,A., De Wit,P.,
731 Sánchez-García,M., Ebersberger,I., de Sousa,F., *et al.* (2013) Improved software detection
732 and extraction of ITS1 and ITS2 from ribosomal ITS sequences of fungi and other
733 eukaryotes for analysis of environmental sequencing data. *Methods Ecol. Evol.*, **4**, 914–919.
734 35. Kumar,S., Stecher,G., Li,M., Knyaz,C. and Tamura,K. (2018) MEGA X: Molecular
735 evolutionary genetics analysis across computing platforms. *Mol. Biol. Evol.*,
736 10.1093/molbev/msy096.
737 36. Rédei,G.P. (2008) CLUSTAL W (improving the sensitivity of progressive multiple sequence
738 alignment through sequence weighting, position-specific gap penalties and weight matrix
739 choice). In *Encyclopedia of Genetics, Genomics, Proteomics and Informatics*.
740 37. Jovanovic,N. and Mikheyev,A.S. (2019) Interactive web-based visualization and sharing of
741 phylogenetic trees using phylogeny.IO. *Nucleic Acids Res.*, **47**, W266–W269.
742 38. Huerta-Cepas,J., Serra,F. and Bork,P. (2016) ETE 3: Reconstruction, Analysis, and
743 Visualization of Phylogenomic Data. *Mol. Biol. Evol.*, **33**, 1635–1638.
744 39. Pryszcz,L.P. and Gabaldón,T. (2016) Redundans: An assembly pipeline for highly
745 heterozygous genomes. *Nucleic Acids Res.*, **44**, e113.
746 40. Camacho,C., Coulouris,G., Avagyan,V., Ma,N., Papadopoulos,J., Bealer,K. and
747 Madden,T.L. (2009) BLAST+: Architecture and applications. *BMC Bioinformatics*, **10**,
748 421.
749 41. Cantarel,B.L., Korf,I., Robb,S.M.C., Parra,G., Ross,E., Moore,B., Holt,C., Alvarado,A.S.
750 and Yandell,M. (2008) MAKER: An easy-to-use annotation pipeline designed for emerging
751 model organism genomes. *Genome Res.*, **18**, 188–196.

752 42. Tarailo-Graovac,M. and Chen,N. (2009) Using RepeatMasker to identify repetitive elements
753 in genomic sequences. *Curr. Protoc. Bioinforma.*, 10.1002/0471250953.bi0410s25.
754 43. Bateman,A., Martin,M.J., O'Donovan,C., Magrane,M., Alpi,E., Antunes,R., Bely,B.,
755 Bingley,M., Bonilla,C., Britto,R., *et al.* (2017) UniProt: The universal protein
756 knowledgebase. *Nucleic Acids Res.*, 10.1093/nar/gkw1099.
757 44. Mi,H. and Thomas,P. (2009) PANTHER pathway: an ontology-based pathway database
758 coupled with data analysis tools. *Methods Mol. Biol.*, **563**, 123–140.
759 45. Ashburner,M., Ball,C.A., Blake,J.A., Botstein,D., Butler,H., Cherry,J.M., Davis,A.P.,
760 Dolinski,K., Dwight,S.S., Eppig,J.T., *et al.* (2000) Gene ontology: Tool for the unification
761 of biology. *Nat. Genet.*, **25**, 25–29.
762 46. Quevillon,E., Silventoinen,V., Pillai,S., Harte,N., Mulder,N., Apweiler,R. and Lopez,R.
763 (2005) InterProScan: Protein domains identifier. *Nucleic Acids Res.*, **33**.
764 47. Hulo,N. (2004) Recent improvements to the PROSITE database. *Nucleic Acids Res.*,
765 10.1093/nar/gkh044.
766 48. Marchler-Bauer,A., Zheng,C., Chitsaz,F., Derbyshire,M.K., Geer,L.Y., Geer,R.C.,
767 Gonzales,N.R., Gwadz,M., Hurwitz,D.I., Lanczycki,C.J., *et al.* (2013) CDD: Conserved
768 domains and protein three-dimensional structure. *Nucleic Acids Res.*, 10.1093/nar/gks1243.
769 49. Finn,R.D., Bateman,A., Clements,J., Coggill,P., Eberhardt,R.Y., Eddy,S.R., Heger,A.,
770 Hetherington,K., Holm,L., Mistry,J., *et al.* (2014) Pfam: The protein families database.
771 *Nucleic Acids Res.*, 10.1093/nar/gkt1223.
772 50. Haft,D.H., Selengut,J.D. and White,O. (2003) The TIGRFAMs database of protein families.
773 *Nucleic Acids Res.*, 10.1093/nar/gkg128.
774 51. Potter,S.C., Luciani,A., Eddy,S.R., Park,Y., Lopez,R. and Finn,R.D. (2018) HMMER web
775 server: 2018 update. *Nucleic Acids Res.*, **46**, W200–W204.
776 52. Almagro Armenteros,J.J., Tsirigos,K.D., Sønderby,C.K., Petersen,T.N., Winther,O.,
777 Brunak,S., von Heijne,G. and Nielsen,H. (2019) SignalP 5.0 improves signal peptide
778 predictions using deep neural networks. *Nat. Biotechnol.*, **37**, 420–423.
779 53. Käll,L., Krogh,A. and Sonnhammer,E.L.L. (2007) Advantages of combined transmembrane
780 topology and signal peptide prediction-the Phobius web server. *Nucleic Acids Res.*, **35**.
781 54. Emanuelsson,O., Brunak,S., von Heijne,G. and Nielsen,H. (2007) Locating proteins in the
782 cell using TargetP, SignalP and related tools. *Nat. Protoc.*, **2**, 953–971.

783 55. Sperschneider,J., Gardiner,D.M., Dodds,P.N., Tini,F., Covarelli,L., Singh,K.B.,
784 Manners,J.M. and Taylor,J.M. (2016) EffectorP: Predicting fungal effector proteins from
785 secretomes using machine learning. *New Phytol.*, **210**, 743–761.
786 56. Zhang,H., Yohe,T., Huang,L., Entwistle,S., Wu,P., Yang,Z., Busk,P.K., Xu,Y. and Yin,Y.
787 (2018) DbCAN2: A meta server for automated carbohydrate-active enzyme annotation.
788 *Nucleic Acids Res.*, **46**, W95–W101.
789 57. Farrer,R.A. (2017) Synima: A Synteny imaging tool for annotated genome assemblies. *BMC*
790 *Bioinformatics*, **18**, 507.
791 58. Li,L., Stoeckert,C.J. and Roos,D.S. (2003) OrthoMCL: Identification of ortholog groups for
792 eukaryotic genomes. *Genome Res.*, **13**, 2178–2189.
793 59. Yu,Y., Ouyang,Y. and Yao,W. (2018) ShinyCircos: An R/Shiny application for interactive
794 creation of Circos plot. *Bioinformatics*, 10.1093/bioinformatics/btx763.
795 60. Krzywinski,M., Schein,J., Birol,I., Connors,J., Gascoyne,R., Horsman,D., Jones,S.J. and
796 Marra,M.A. (2009) Circos: An information aesthetic for comparative genomics. *Genome*
797 *Res.*, 10.1101/gr.092759.109.
798 61. Alexa,A. and Rahnenführer,J. (2009) Gene set enrichment analysis with topGO.
799 *Bioconductor Improv*, **27**.
800 62. Marçais,G., Delcher,A.L., Phillippy,A.M., Coston,R., Salzberg,S.L. and Zimin,A. (2018)
801 MUMmer4: A fast and versatile genome alignment system. *PLoS Comput. Biol.*, **14**.
802 63. Cubeta,M.A., Thomas,E., Dean,R.A., Jabaji,S., Neate,S.M., Tavantzis,S., Toda,T.,
803 Vilgalys,R., Bharathan,N., Fedorova-Abrams,N., *et al.* (2014) Draft genome sequence of
804 the plant-pathogenic soil fungus Rhizoctonia solani anastomosis group 3 strain Rhs1AP.
805 *Genome Announc.*, 10.1128/genomeA.01072-14.
806 64. Lakshman,D.K., Liu,C., Mishra,P.K. and Tavantzis,S. (2006) Characterization of the arom
807 gene in Rhizoctonia solani, and transcription patterns under stable and induced
808 hypovirulence conditions. *Curr. Genet.*, 10.1007/s00294-005-0005-6.
809 65. Lamb,H.K., Van Den Hombergh,J.P.T.W., Newton,G.H., Moore,J.D., Roberts,C.F. and
810 Hawkins,A.R. (1992) Differential flux through the quinate and shikimate pathways:
811 Implications for the channelling hypothesis. *Biochem. J.*, 10.1042/bj2840181.
812 66. Lakshman,D.K., Jian,J. and Tavantzis,S.M. (1998) A double-stranded RNA element from a
813 hypovirulent strain of Rhizoctonia solani occurs in DNA form and is genetically related to

814 the pentafunctional AROM protein of the shikimate pathway. *Proc. Natl. Acad. Sci. U. S.*
815 *A.*, **95**, 6425–6429.
816 67. Črešnar,B. and Petrič,Š. (2011) Cytochrome P450 enzymes in the fungal kingdom. *Biochim.*
817 *Biophys. Acta - Proteins Proteomics*, 10.1016/j.bbapap.2010.06.020.
818 68. Kim,K.T., Jeon,J., Choi,J., Cheong,K., Song,H., Choi,G., Kang,S. and Lee,Y.H. (2016)
819 Kingdom-wide analysis of fungal small secreted proteins (SSPs) reveals their potential role
820 in host association. *Front. Plant Sci.*, **7**.
821 69. McCotter,S.W., Horianopoulos,L.C. and Kronstad,J.W. (2016) Regulation of the fungal
822 secretome. *Curr. Genet.*, **62**, 533–545.
823 70. Li,T., Wu,Y., Wang,Y., Gao,H., Gupta,V.K., Duan,X., Qu,H. and Jiang,Y. (2019) Secretome
824 profiling reveals virulence-associated proteins of Fusarium proliferatum during interaction
825 with banana fruit. *Biomolecules*, **9**.
826 71. Linder,M., Lindeberg,G., Reinikainen,T., Teeri,T.T. and Pettersson,G. (1995) The difference
827 in affinity between two fungal cellulose-binding domains is dominated by a single amino
828 acid substitution. *FEBS Lett.*, 10.1016/0014-5793(95)00961-8.
829 72. Stergiopoulos,I. and de Wit,P.J.G.M. (2009) Fungal Effector Proteins. *Annu. Rev.*
830 *Phytopathol.*, **47**, 233–263.
831 73. Wei,M., Wang,A., Liu,Y., Ma,L., Niu,X. and Zheng,A. (2020) Identification of the Novel
832 Effector RsIA_NP8 in Rhizoctonia solani AG1 IA That Induces Cell Death and Triggers
833 Defense Responses in Non-Host Plants. *Front. Microbiol.*, 10.3389/fmicb.2020.01115.
834 74. Yamamoto,N., Wang,Y., Lin,R., Liang,Y., Liu,Y., Zhu,J., Wang,L., Wang,S., Liu,H.,
835 Deng,Q., *et al.* (2019) Integrative transcriptome analysis discloses the molecular basis of a
836 heterogeneous fungal phytopathogen complex, Rhizoctonia solani AG-1 subgroups. *Sci.*
837 *Rep.*, **9**.
838 75. Kameshwar,A.K.S., Ramos,L.P. and Qin,W. (2019) CAZymes-based ranking of fungi
839 (CBRF): an interactive web database for identifying fungi with extrinsic plant biomass
840 degrading abilities. *Bioresour. Bioprocess.*, 10.1186/s40643-019-0286-0.
841 76. Barrett,K., Jensen,K., Meyer,A.S., Frisvad,J.C. and Lange,L. (2020) Fungal secretome
842 profile categorization of CAZymes by function and family corresponds to fungal phylogeny
843 and taxonomy: Example Aspergillus and Penicillium. *Sci. Rep.*, 10.1038/s41598-020-
844 61907-1.

845 77. Lombard,V., Golaconda Ramulu,H., Drula,E., Coutinho,P.M. and Henrissat,B. (2014) The
846 carbohydrate-active enzymes database (CAZy) in 2013. *Nucleic Acids Res.*,
847 10.1093/nar/gkt1178.
848 78. Henrissat,B. (1991) A classification of glycosyl hydrolases based on amino acid sequence
849 similarities. *Biochem. J.*, 10.1042/bj2800309.
850 79. Wibberg,D., Genzel,F., Verwaaijen,B., Blom,J., Rupp,O., Goesmann,A., Zrenner,R.,
851 Grosch,R., Pühler,A. and Schlüter,A. (2017) Draft genome sequence of the potato pathogen
852 Rhizoctonia solani AG3-PT isolate Ben3. *Arch. Microbiol.*, **199**, 1065–1068.
853 80. Wibberg,D., Andersson,L., Rupp,O., Goesmann,A., Pühler,A., Varrelmann,M., Dixelius,C.
854 and Schlüter,A. (2016) Draft genome sequence of the sugar beet pathogen Rhizoctonia
855 solani AG2-2IIIB strain BBA69670. *J. Biotechnol.*, 10.1016/j.jbiotec.2016.02.001.
856 81. Wibberg,D., Rupp,O., Jelonek,L., Kröber,M., Verwaaijen,B., Blom,J., Winkler,A.,
857 Goesmann,A., Grosch,R., Pühler,A., *et al.* (2015) Improved genome sequence of the
858 phytopathogenic fungus Rhizoctonia solani AG1-IB 7/3/14 as established by deep mate-pair
859 sequencing on the MiSeq (Illumina) system. *J. Biotechnol.*, 10.1016/j.jbiotec.2015.03.005.
860 82. Richard W. Smiley, Peter H. Dernoeden, and B.B.C. (2005) Compendium of Turfgrass
861 Diseases, Third Edition.
862 83. Burpee,L.L. and Martin,S.B. (1996) Biology of Turfgrass Diseases Incited by Rhizoctonia
863 Species. In *Rhizoctonia Species: Taxonomy, Molecular Biology, Ecology, Pathology and*
864 *Disease Control*.
865 84. Amaradasa,B.S., Lakshman,D., Mccall,D.S. and Horvath,B.J. (2014) In Vitro Fungicide
866 Sensitivity of Rhizoctonia and Waitea Isolates Collected from Turfgrasses 1.
867 85. Campion,C., Chatot,C., Perraton,B. and Andrivon,D. (2003) Anastomosis groups,
868 pathogenicity and sensitivity to fungicides of Rhizoctonia solani isolates collected on potato
869 crops in France. *Eur. J. Plant Pathol.*, 10.1023/B:EJPP.0000003829.83671.8f.
870 86. Bernard,E., Larkin,R.P., Tavantzis,S., Erich,M.S., Alyokhin,A., Sewell,G., Lannan,A. and
871 Gross,S.D. (2012) Compost, rapeseed rotation, and biocontrol agents significantly impact
872 soil microbial communities in organic and conventional potato production systems. *Appl.*
873 *Soil Ecol.*, 10.1016/j.apsoil.2011.10.002.
874 87. Roberts,D.P. and Kobayashi,D.Y. (2011) Impact of Spatial Heterogeneity Within
875 Spermosphere and Rhizosphere Environments on Performance of Bacterial Biological

876 Control Agents. In *Bacteria in Agrobiology: Crop Ecosystems*.
877 88. Roper,M., Simonin,A., Hickey,P.C., Leeder,A. and Glass,N.L. (2013) Nuclear dynamics in a
878 fungal chimera. *Proc. Natl. Acad. Sci. U. S. A.*, 10.1073/pnas.1220842110.
879 89. Liu,C., Lakshman,D.K. and Tavantzis,S.M. (2003) Quinic acid induces hypovirulence and
880 expression of a hypovirulence-associated double-stranded RNA in Rhizoctonia solani. *Curr.*
881 *Genet.*, 10.1007/s00294-003-0375-6.
882 90. Van Bueren,A.L., Morland,C., Gilbert,H.J. and Boraston,A.B. (2005) Family 6 carbohydrate
883 binding modules recognize the non-reducing end of β-1,3-linked glucans by presenting a
884 unique ligand binding surface. *J. Biol. Chem.*, 10.1074/jbc.M410113200.
885 91. Fochi,V., Chitarra,W., Kohler,A., Voyron,S., Singan,V.R., Lindquist,E.A., Barry,K.W.,
886 Girlanda,M., Grigoriev,I. V., Martin,F., *et al.* (2017) Fungal and plant gene expression in
887 the Tulasnella calospora–Serapias vomeracea symbiosis provides clues about nitrogen
888 pathways in orchid mycorrhizas. *New Phytol.*, 10.1111/nph.14279.
889 92. Harrison,P.W., Alako,B., Amid,C., Cerdeño-Tárraga,A., Cleland,I., Holt,S., Hussein,A.,
890 Jayathilaka,S., Kay,S., Keane,T., *et al.* (2019) The European Nucleotide Archive in 2018.
891 *Nucleic Acids Res.*, 10.1093/nar/gky1078.
892 93. Leinonen,R., Akhtar,R., Birney,E., Bower,L., Cerdeno-Tárraga,A., Cheng,Y., Cleland,I.,
893 Faruque,N., Goodgame,N., Gibson,R., *et al.* (2011) The European nucleotide archive.
894 *Nucleic Acids Res.*, 10.1093/nar/gkq967.
895

Figure legends

Figure 1. A. **Circos plot**. The Circos plot represents the syntenic relationship between genomes of the different AGs of *Rhizoctonia solani* Kühn. Each line represents the region of genomic similarity predicted with Synima. Only the regions with coverage > 40,000 bases were enumerated and shown. B**.** The plot highlights the number of high-similarity syntenic regions (coverage > 40,000 bp) shared between each pair of genomes, including *T. calospora*. The red connection represents corresponding isolates sharing comparatively large number of syntenic relationships than other pair of isolates. Here, self-hits were removed or not shown. C. **ITS2 phylogeny**. ITS2 sequences of the tester strain were obtained from the NCBI database and were clustered with ITS2 sequences from assembled *R. solani* genomes (highlighted with blue color and *), along with ITS2 sequences from previously published *R. solani* genome assemblies (marked with **). The phylogenetic tree was constructed using megax software with 10,000 bootstrapping steps (see methods), after which resulting tree and corresponding alignment were visualized together using Phylogeny.IO.

Figure 2. orthoMCL clustering of the predicted proteomes in *R. solani* AGs. A. Heatmap showing protein conservation across all sequenced *R. solani* AGs and *T. calospora*. Each row represents one orthoMCL cluster, and color is proportional to the number of protein members shared within a given cluster from the given species (black: no member protein present; red: large number of protein members present). The hierarchical clustering (hclust; method: complete) analysis enumerates the similarities between different fungal isolates based on proteins shared by them across all orthoMCL clusters. B. **Cluster frequency**. The line plot represents the number of orthoMCL clusters shared by different fungal isolates used in this study. Example, > 1400 orthoMCL clusters are shared by 14 different fungal isolates (including

919 positive and negative controls) used in this study. The bimodal nature of plot represent high
920 similarities across independent proteomes as large number of clusters shares protein members
921 from ≥13 fungal isolates. The red line represents the smoothed curves after averaging out the
922 number of clusters. C. **Protein classification based on the orthoMCL clusters**. The "core"
923 proteins represent the sub-set of proteomes (from each *R. solani* AG and *T. calospsora*) with
924 conserved profile across all the isolates. Similarly, the "unique" sets represent the isolate-specific
925 protein subset. The rest of the protein subsets make the "Auxillary" proteome which are
926 conserved in a limited number of isolates. D. **Shared orthoMCL clusters**. The number of
927 orthoMCL clusters shared between any two isolates. A shared cluster means, a given orthoMCL
928 cluster contains proteins from both the isolates.

929 **Figure 3**. **InterPro domain analysis of the unique proteome**. In the unique proteome of each
930 fungal isolate, InterPro protein domain families were predicted using InterProScan (Version
931 5.45-80.0). Only the top 5 most enriched protein families are shown. The number marks the
932 corresponding annotation of InterPro family domain in the circular bar plot.

933 **Figure 4**. **The Secreted Proteins**. A. Number of predicted proteins in the secretome of each
934 fungal isolate (highlighted in yellow)**.** The secreted proteins predicted in the unique proteome of
935 each isolate is highlighted in red. B. Comparative analysis of top six highly enriched InterPro
936 domains in the secretome.

937 **Figure 5**. **Effector Proteins.** A. The number of cysteine rich effector proteins predicted in the
938 predicted secretome of each fungal isolate. B. The proportion of Cysteine observed across all the
939 effectors predicted in each isolate. C. Topmost Enriched InterPro domains in Effector proteins of
940 Rhizoctonia species (not *T. calospora*) and other basidiomycetes (including *T. calospora*). D.
941 The comparative analysis of the distribution of number of effector proteins predicted in *R. solani*

942 AGs as compared to other Basidiomycetes. The p-value is computed using unpaired Wilcoxon-
943 rank sum test.

944 **Figure 6**. **CAZymes**. A. The number of carbohydrate metabolizing enzymes (CAZymes)
945 predicted in the proteome of each fungal isolate. B. Heatmap showing the CAZyme conservation
946 across all the *R. solani* AGs and *T. calospora*. Each row represents one CAZy family of proteins,
947 and color is proportional to the number of protein members shared within a given family from
948 the given species (black: no member protein present; red: large number of protein members
949 present). The hierarchical clustering (hclust; method: complete) enumerates the similarities
950 between different fungal isolates based on proteins shared by them across all CAZy families. For
951 simplicity only the CAZyme families enriched in more than 50 enzymes across all proteomes are
952 shown.

953

Figure 1

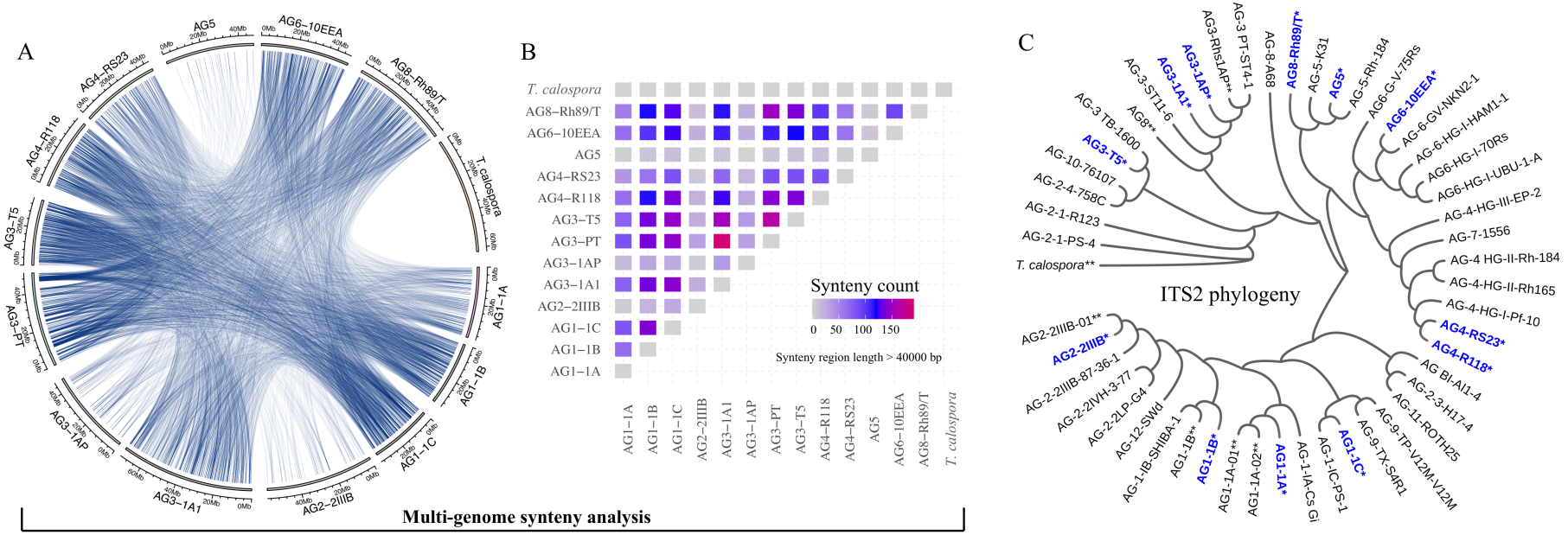

Multi-genome synteny analysis

954

955

Figure 2

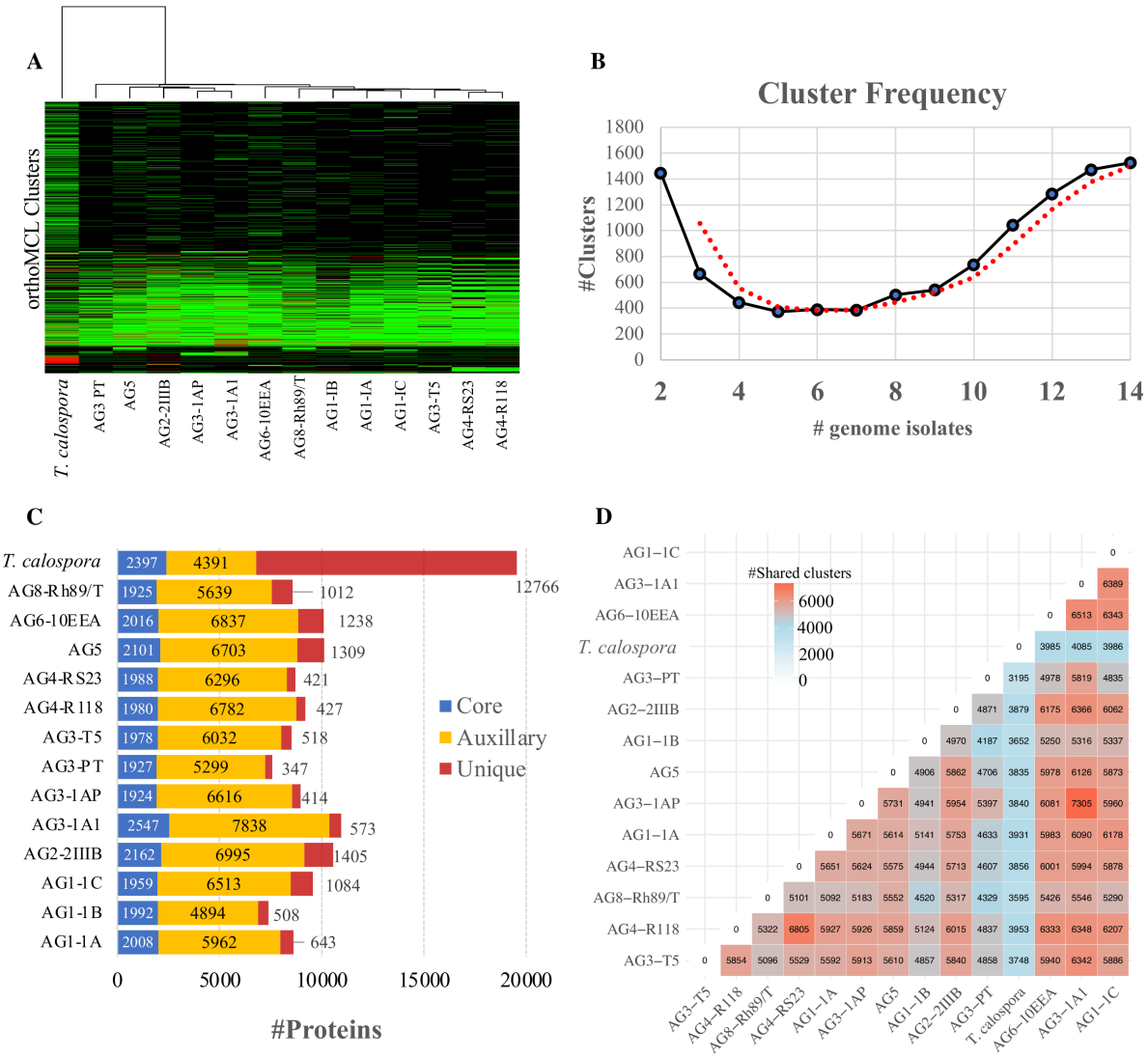

957

958

959

Figure 3

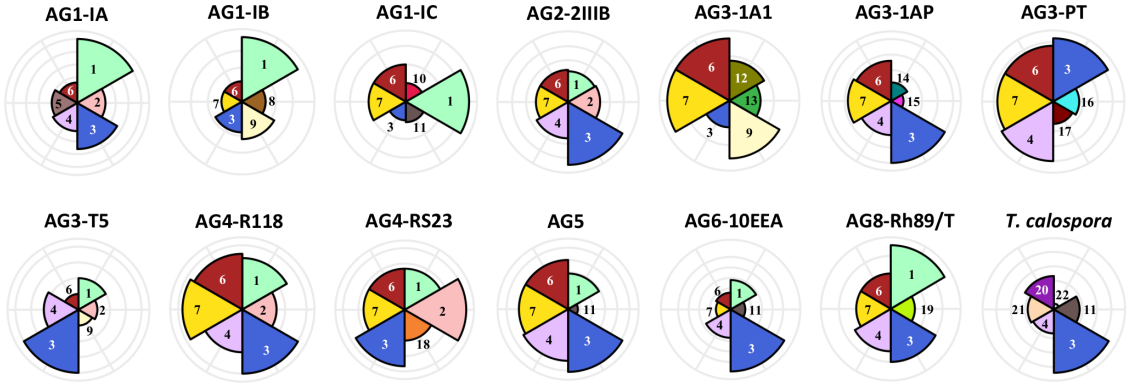

InterPro Domains

1	Cytochrome P450
2	Fungal Transcription Factor
3	Protein Kinase Domain
4	Serine-threonine/tyrosine protein kinase catalytic domain
5	Short chain dehydrogenase/reductase SDR
6	WD40 repeat containing domain
7	WD40 repeat
8	NADH: Flavin Oxidoreductase/ NADH oxidase (N-terminal)
9	NADP-dependent oxidoreductase domain
10	BTB/POZ domain
11	F-box domain
12	ABC transporter-like
13	Aminoacyl-tRNA synthetase (class-II)
14	Multicopper oxidase (Type 2)
15	Patatin like phospholipase domain
16	Ribosomal protein S4/S9
17	Ribosomal protein S4/S9 (Eukaryotic/Archaeal)
18	Major facilitator superfamily domain
19	Lysine-specific metallo-endopeptidase
20	Tetratricopeptide repeat-containing domain
21	Tetratricopeptide repeat
22	Cytochrome P50

960

961

962

Figure 4

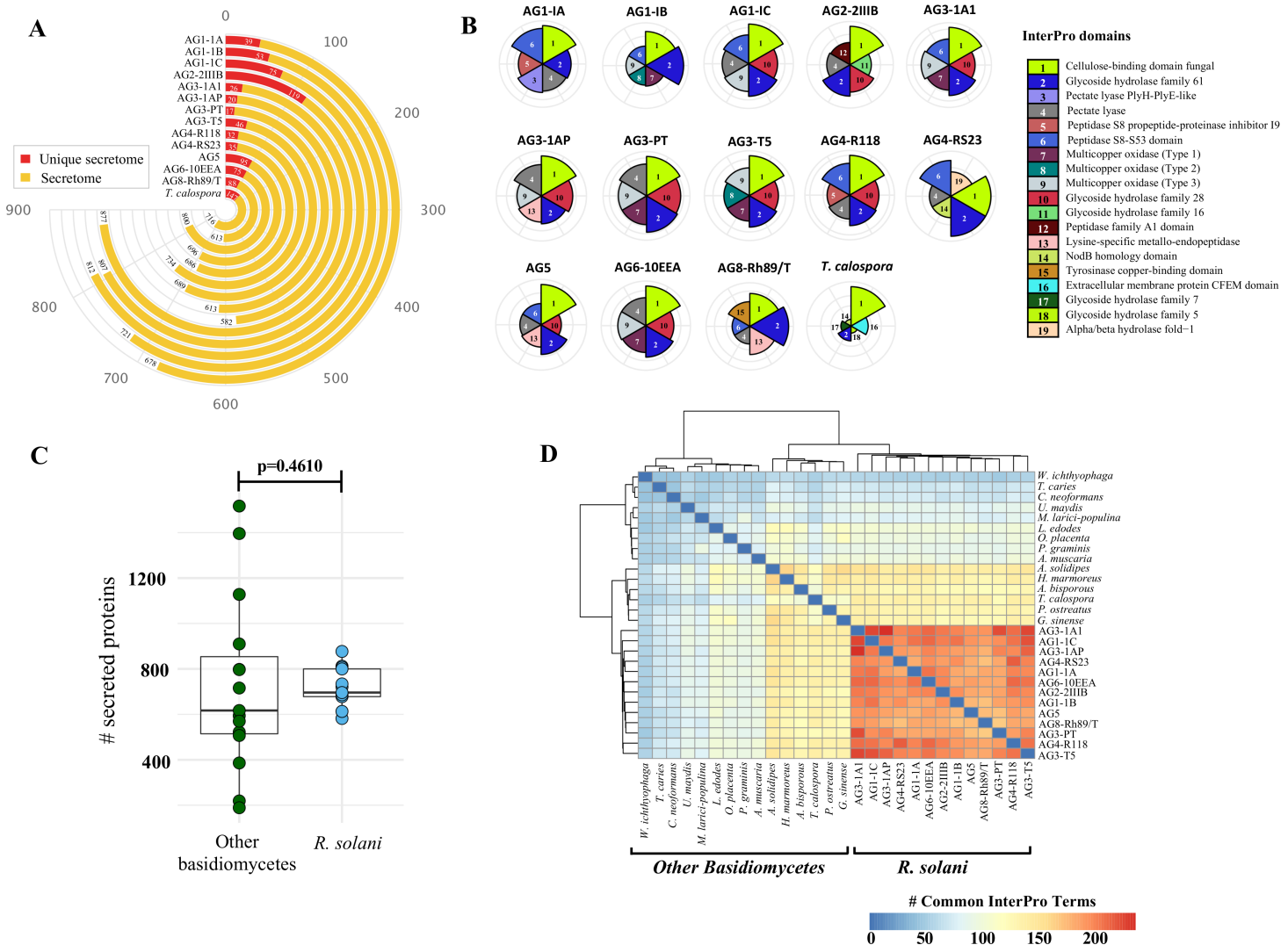

963

964

Figure 5

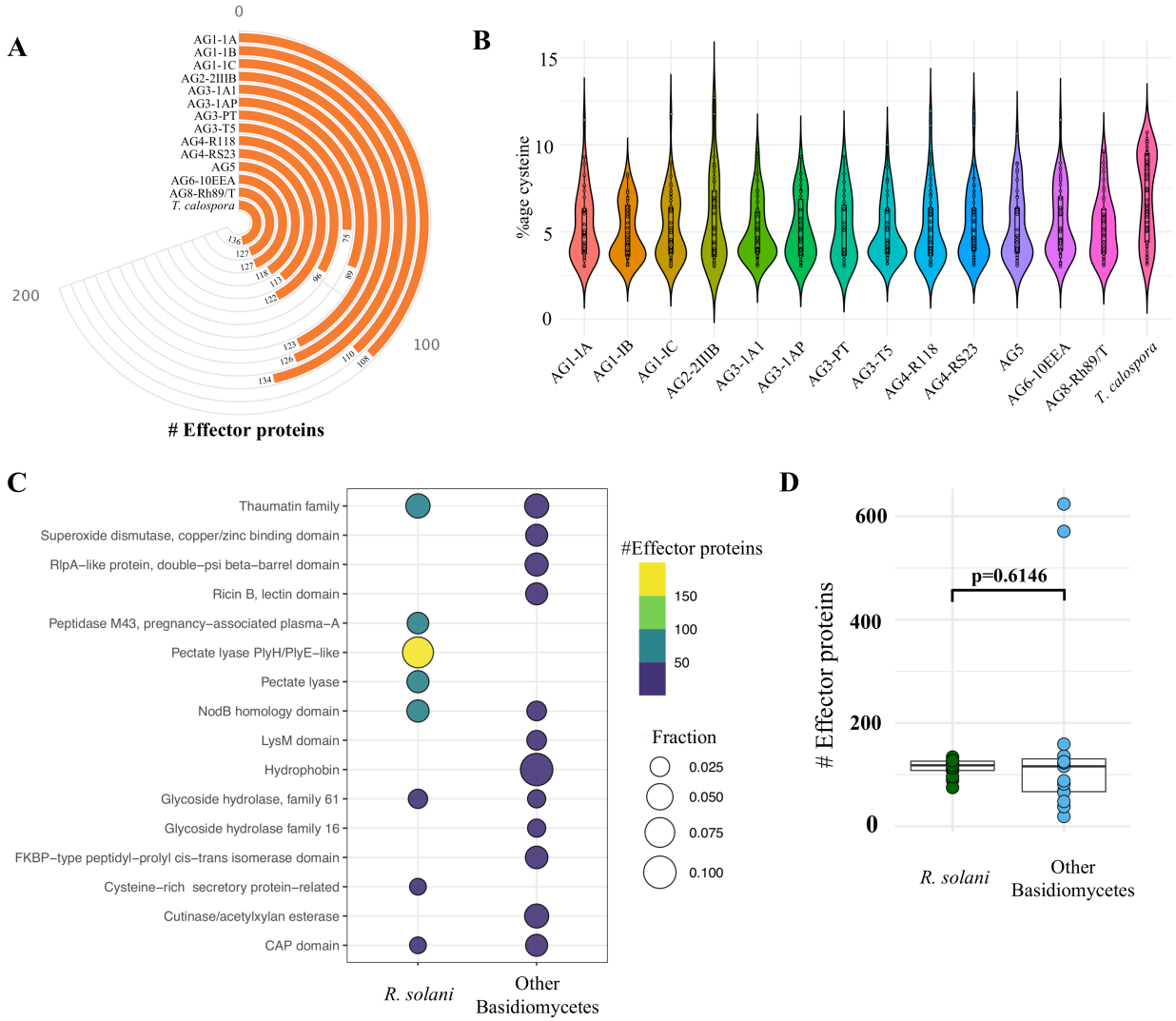

965

966

Figure 6

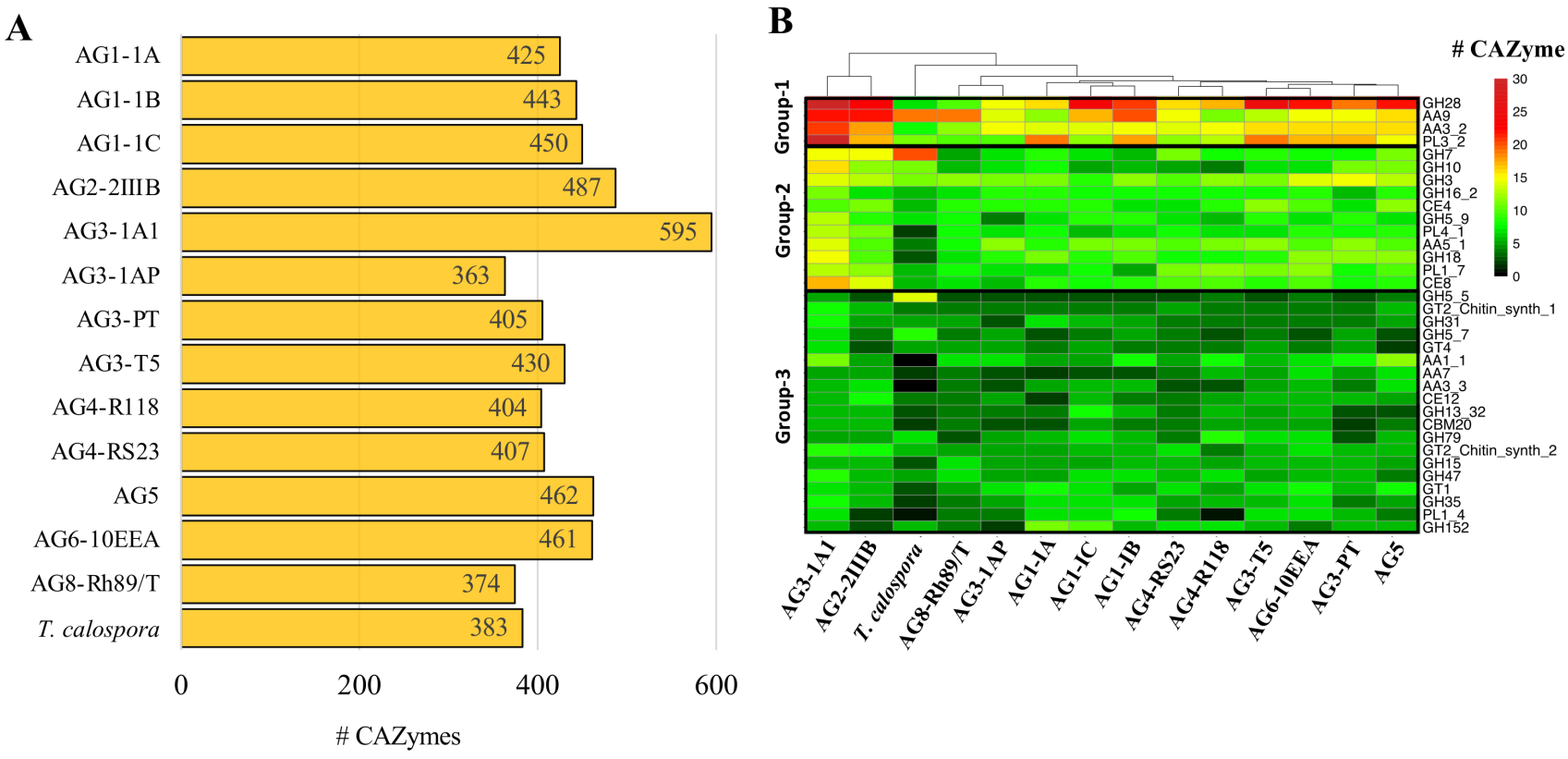

967

968

969